Nonlinear dispersion-based incoherent photonic processing for microwave pulse generation with full reconfigurability

Mario Bolea, José Mora,* Beatriz Ortega, and José Capmany

ITEAM Research Institute, Universidad Politécnica de Valencia, C/ Camino de Vera, s/n 46022 Valencia Spain
**jmalmer@iteam.upv.es*

Abstract: A novel all-optical technique based on the incoherent processing of optical signals using high-order dispersive elements is analyzed for microwave arbitrary pulse generation. We show an approach which allows a full reconfigurability of a pulse in terms of chirp, envelope and central frequency by the proper control of the second-order dispersion and the incoherent optical source power distribution, achieving large values of time-bandwidth product.

OCIS codes: (060.0060) Fiber optics and optical communications; (060.5625) Radio frequency photonics.

References and links

1. J. Capmany and D. Novak, "Microwave photonics combines two worlds," Nat. Photonics **1**(6), 319–330 (2007).
2. J. Yao, "Microwave photonics: *a*rbitrary waveform generation," Nat. Photonics **4**(2), 79–80 (2010).
3. J. Yao, "Photonic generation of microwave arbitrary waveforms," Opt. Commun. **284**(15), 3723–3736 (2011).
4. C.-B. Huang and A. M. Weiner, "Analysis of time-multiplexed optical line-by-line pulse shaping: application for radio-frequency and microwave photonics," Opt. Express **18**(9), 9366–9377 (2010).
5. V. Torres-Company, J. Lancis, and P. Andrés, "Incoherent frequency-to-time mapping: application to incoherent pulse shaping," J. Opt. Soc. Am. A **24**(3), 888–894 (2007).
6. V. Torres-Company, J. Lancis, P. Andrés, and L. R. Chen, "20 GHz arbitrary radio-frequency waveform generator based on incoherent pulse shaping," Opt. Express **16**(26), 21564–21569 (2008).
7. M. Bolea, J. Mora, B. Ortega, and J. Capmany, "Photonic arbitrary waveform generation applicable to multiband UWB communications," Opt. Express **18**(25), 26259–26267 (2010).
8. J. G. Proakis, *Digital Communications*, 3rd ed. (McGraw-Hill, Singapore, 1995).
9. M. Skolnik, *Radar Handbook*, 3rd ed. (McGraw-Hill, United States of America, 2008).
10. M. Bertero, M. Miyakawa, P. Boccacci, F. Conte, K. Orikasa, and M. Furutani, "Image restoration in chirp-pulse microwave CT (CP-MCT)," IEEE Trans. Biomed. Eng. **47**(5), 690–699 (2000).
11. C. Wang and J. Yao, "Photonic generation of chirped millimeter-wave pulses based on nonlinear frequency-to-time mapping in a nonlinearly chirped fiber Bragg *g*rating," IEEE Trans. Microw. Theory Tech. **56**(2), 542–553 (2008).
12. H. Chi and J. Yao, "All-fiber chirped microwave pulses generation based on spectral shaping and wavelength-to-time conversion," IEEE Trans. Microw. Theory Tech. **55**(9), 1958–1963 (2007).
13. C. Wang and J. Yao, "Chirped microwave pulse generation based on optical spectral shaping and wavelength-to-time mapping using a Sagnac-loop mirror incorporating a chirped fiber Bragg grating," J. Lightwave Technol. **27**(16), 3336–3341 (2009).
14. Y. Park and J. Azaña, "Ultrahigh dispersion of broadband microwave signals by incoherent photonic processing," Opt. Express **18**(14), 14752–14761 (2010).
15. M. Bolea, J. Mora, B. Ortega, and J. Capmany, "Reconfigurability and tunability of a chirped microwave photonic pulse generator," *Proceedings on Microwave Photonic 2010*, (Montreal 2010), pp. 167–170.
16. J. W. Shi, F. M. Kuo, N. W. Chen, S. Y. Set, C. B. Huang, and J. E. Bowers, "Photonic generation and wireless transmission of linearly/nonlinearly continuously tunable chirped millimeter-wave waveforms with high time-bandwidth product at W-band," IEEE Photon. J. **4**(1), 215–223 (2012).
17. C. Dorrer, "Statistical analysis of incoherent pulse shaping," Opt. Express **17**(5), 3341–3352 (2009).
18. A. M. Vengsarkar and I. M. Besieris, "Regenerative periodic pulse trains in linear, single-mode optical fibers: effect of finite source linewidths," IEEE Photon. Technol. Lett. **3**(1), 33–35 (1991).
19. S. Shin, U. Sharma, H. Tu, W. Jung, and S. A. Boppart, "Characterization and analysis of relative intensity noise in broadband optical sources for optical coherence tomography," IEEE Photon. Technol. Lett. **22**(14), 1057–1059 (2010).

#162085 - $15.00 USD Received 25 Jan 2012; revised 13 Feb 2012; accepted 17 Feb 2012; published 7 Mar 2012

20. Y. Park, A. Malacarne, and J. Azaña, "Real-time ultrawide-band group delay profile monitoring through low-noise incoherent temporal interferometry," Opt. Express **19**(5), 3937–3944 (2011).
21. C. Pulikkaseril, "Filter Bandwidth Definition of the WaveShaper S-series Programmable Processor," Finisar product whitepaper.
22. C. B. Huang, D. E. Leaird, and A. M. Weiner, "Time-multiplexed photonically enabled radio-frequency arbitrary waveform generation with 100 ps transitions," Opt. Lett. **32**(22), 3242–3244 (2007).
23. C. M. Long, D. E. Leaird, and A. M. Weiner, "Photonically enabled agile rf waveform generation by optical comb shifting," Opt. Lett. **35**(23), 3892–3894 (2010).

1. Introduction

Photonically assisted Arbitrary Waveform Generation (AWG) allows frequency operation ranges of tens of GHz in contrast with pure electronic systems restricted close to 10 GHz. The ability to generate high frequency and large bandwidth signals becomes extremely important in different application fields such as: radar systems, wireless communications, software defined radio and modern instrumentation [1, 2]. Currently, a great number of approaches related to microwave AWG in the optical domain have been proposed including direct space-to-time pulse shaping, temporal pulse shaping, optical spectral shaping combined with frequency-to-time mapping [3], optical line-by-line intensity and phase modulation [4], incoherent pulse shaping [5, 6] and microwave photonic filtering [7].

In particular, photonic schemes designed to generate chirped microwave pulses have a special interest since can be achieved featuring a broad frequency operation range and high values of time-bandwidth product (TBWP). Several applications benefit from these features, such as spread spectrum communications, pulsed compression radars or tomography for medical imaging [8–10]. Firstly, a coherent nonlinear frequency-to-time mapping in a high-order dispersive element was proposed [11, 12]. In this case, TBWP depends on the second-order dispersion so this technique is experimentally limited to a TBWP value of 4. In order to increase this product, other approaches propose to achieve a chirped behaviour by means of a optical source slicing obtaining TBWP values around 40 [13]. A drawback of these techniques consists on the lack of flexibility to experimentally reconfigure the output waveform. Therefore, incoherent source processing systems have been also proposed to generate chirped arbitrary waveforms with large TBWP [14]. Nevertheless, in this case, the arbitrariness of the generated signal is restricted, since the waveform envelope is electrically controlled. In order to increase the waveform flexibility, we recently proposed a photonic scheme that allows both optical arbitrary waveform generation and large TBWP by the processing of an incoherent optical signal using a nonlinear dispersive element which experimental results were reported in [15]. Recently, a high TBWP of several hundreds of thousands has been experimentally demonstrated by a heterodyne-beating using two lasers [16]. However, this system is drastically restricted to low rates (~kb/s) because of the sweep time of lasers dependence. In contrast, the previous systems based on coherent or incoherent optical processing permit to achieve high rates (hundreds of Mb/s) which are required in a lot of applications.

The main restriction of incoherent light processing systems is related to a low signal-to-noise ratio [17]. In the structures with incoherent sources proposed for AWG, this fact gives as a result intensity fluctuations of the optical field associated to the generated output waveform [5, 6, 14]. In order to avoid this limitation a proper average of the generated signal can be carried out [7]. Moreover, the use of a differential photodetection has been experimentally demonstrated to achieve a significant improvement in the signal-to-noise ratio of the generated waveform reducing the number of required averaging events [14, 15].

In this paper, we propose and analyze a novel technique based on incoherent signal processing which employs nonlinear dispersive element and which is adaptable to achieve chirped arbitrary waveforms. We have carried out several numerical simulations of the proposed system in order to show different capabilities in terms of chirp, frequency and envelope of the generated waveform. To the best of our knowledge, this is the first structure

#162085 - $15.00 USD Received 25 Jan 2012; revised 13 Feb 2012; accepted 17 Feb 2012; published 7 Mar 2012

which operates as an incoherent nonlinear frequency-to-time mapping system where a full reconfigurability can be achieved by controlling the optical source power distribution with a chirp value depending on the second-order dispersion. In particular, the use of realistic parameters corresponding to commercial devices allows to obtain TBWP value around 90.

2. Operation principle

The operation principle of the proposed technique is illustrated in Fig. 1. In our theoretical analysis we consider a broadband optical source which is given by the power spectral density S(ω), centred at ω_o, such that the optical field of the light source describes a stationary random process. As Fig. 1(a) describes, each optical frequency ω' in the broadband spectrum emitted by the optical source is modulated by means of a modulator impulse response $h_{mod}(t)$ which full-width half maximum pulse duration is σ_0, corresponding to an spectral response shown in Fig. 1(b). Then, the modulated signal is launched into an optical processor which is determined by the temporal impulse response $h_{disp}(t)$. As shown in Fig. 1(c), a non-linear dispersive element is used as optical processor which can be described by the optical transfer function $H_{disp}(\omega) = H_o e^{-j\varphi(\omega)}$ where first- and second- order dispersion are considered. Therefore, the phase response φ(ω) can be expanded as:

$$\varphi(\omega) = \varphi_o + \varphi_1\omega + \frac{1}{2!}\varphi_2\omega^2 + \frac{1}{3!}\varphi_3\omega^3 \qquad (1)$$

where φ_1 is the group-delay time at the central optical frequency ω_o and φ_2 and φ_3 are the first- and second-order dispersion, respectively, evaluated at the same frequency. Note that above parameter ω represents the relative optical frequency with respect to the reference optical frequency ω_o and H_o corresponds to the optical losses in the dispersive element.

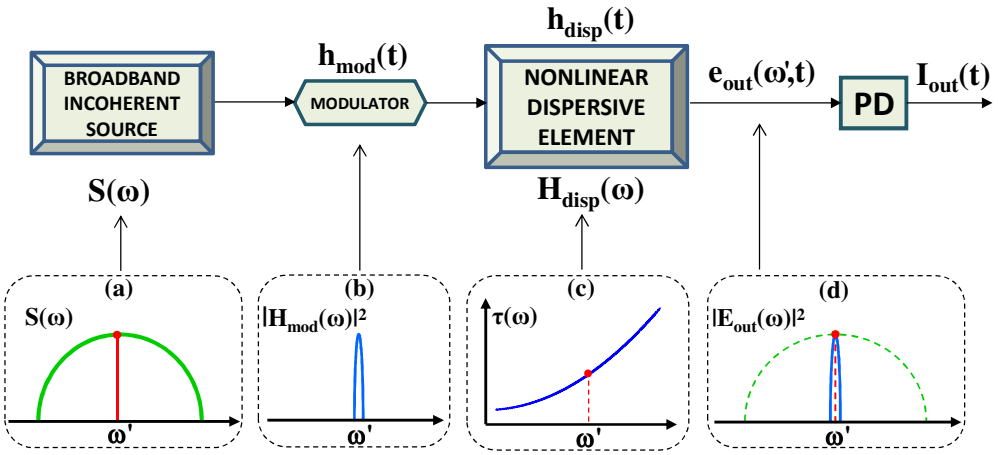

Fig. 1. Schematic diagram of the nonlinear incoherent optical processing technique operating as a microwave pulse generation system. PD: photodetector. Insets: (a) power spectral distribution of the optical source, (b) transfer function of modulator response at angular optical frequency ω', (c) optical delay of high-order dispersive element and (d) power spectral density of modulated signal at ω' after propagation.

After dispersive propagation, the optical field when we consider a monochromatic source centred at the optical frequency ω' is given by:

$$e_{out}(\omega', t) = e^{j\omega' t} \cdot h_{mod}(t) \otimes h_{disp}(t) \qquad (2)$$

Without considering additional assumptions, Fig. 1 represents a conventional electrooptical scheme of an optical carrier with a spectral distribution S(ω) by means of

#162085 - $15.00 USD Received 25 Jan 2012; revised 13 Feb 2012; accepted 17 Feb 2012; published 7 Mar 2012

external modulation and photodetection after propagation through a given optical processor $H_{disp}(\omega)$ [16]. Therefore, the average intensity $I_{out}(t)$ results to be a superposition of monochromatic carrier waves which are spectrally weighted by the optical spectral density $S(\omega)$ previously to dispersive propagation. In this way, according to [18], $I_{out}(t)$ can be obtained as follows:

$$I_{out}(t) = \frac{I_o}{2\pi}\int_{-\infty}^{+\infty} S(\omega)\left|e_{out}(\omega,t)\right|^2 d\omega \tag{3}$$

where I_o includes different system parameters as the optical losses of the nonlinear dispersive element, the responsivity and impedance of the photodetector.

At this point, we assume that the dispersive element satisfies the condition $\sigma_0 \gg \left|\varphi_3 / \varphi_2\right|$ which is verified by dispersive delay lines and electrical pulses commonly used in experiments. As described in Fig. 1(c), this condition implies that second-order dispersion is negligible over the input pulse but not necessarily over the optical source power spectral distribution. In this way, introducing Eq. (1) into Eq. (2) and considering the previous assumption, we can find that the average intensity for each frequency component ω' is given by the average intensity at the optical frequency ω_o which is delayed by the dispersion in the following form:

$$\left|e_{out}(\omega,t)\right|^2 \cong \left|h_{\mathrm{mod}}(\omega_o,t)\right|^2 \otimes \delta\left(t-\tau(\omega)\right) \quad where \quad \tau(\omega) = \varphi_1 + \varphi_2\omega + \frac{1}{2}\varphi_3\omega^2 \tag{4}$$

The parameter $\tau(\omega)$ represents the group time delay for each optical frequency coming from the first-order derivative of Eq. (1) as plotted in Fig. 1(c). Therefore, introducing Eq. (4) into Eq. (3), we can obtain the expression of the generated electrical signal by a contribution which is a sum of incoherent terms given as:

$$I_{OUT}(t) = \frac{I_o}{2\pi}\left.\frac{S(\omega)}{\left|\varphi_2+\varphi_3\omega\right|}\right|_{\omega=\omega_m} \otimes \left|h_{\mathrm{mod}}(\omega_o,t)\right|^2 \qquad with \quad \omega_m(t) = \left|\frac{\varphi_2}{\varphi_3}\right|\left(1-\sqrt{1+2\frac{\varphi_3 t}{\varphi_2^2}}\right) \tag{5}$$

For simplicity, the parameter t represents the relative time with respect to φ_1. From the first term of Eq. (5), we observe that it corresponds with nonlinear frequency-to-time process since the output signal can be considered a time-domain scaled version of the power spectrum $S(\omega)$ with a scale factor given by $\omega_m(t)$. We can see that Eq. (5) corresponds to an extension of the schemes based on linear incoherent optical signal processing in which second-order dispersion is neglected [5, 6]. Indeed, when we consider that φ_3 tends to zero, the scale factor becomes $\omega_m = t/|\varphi_2|$. For a general case, we obtain a nonlinear frequency-to-time relationship between the parameter ω_m and the relative time showing a similar behavior as reported in [12] where a coherent regime is considered. In our case, a difference is found in the first term of Eq. (5) since the equivalent mapping is not only realized over the power spectral density $S(\omega)$ but also it is related to the local dispersion at a given optical frequency ω respect to ω_o. Indeed, the denominator of the first term corresponds to the first-order derivative of the group time delay of Eq. (4).

As we have previously pointed out, the second term of Eq. (5) represents the output pulse when a monochromatic source is considered. For an optimized performance of the nonlinear incoherent processing by enhancing the first term of Eq. (5), we have to compare the pulse duration between both terms to minimize the convolutional effects of the second term over the first one. Taking into account the coherence time σ_c of the optical source which is scaled as shown in Eq. (5) and the input pulsewidth $\sigma_0 \gg \left|\varphi_3 / \varphi_2\right|$, we assume the following conditions which establish the limits to satisfy an optimized nonlinear frequency-to-time process:

#162085 - $15.00 USD Received 25 Jan 2012; revised 13 Feb 2012; accepted 17 Feb 2012; published 7 Mar 2012

$$\left|\varphi_2+\frac{1}{2}\frac{\varphi_3}{\sigma_c}\right| \gg \sigma_0\sigma_c \qquad \sigma_0 \gg \sigma_c \tag{6}$$

From Eq. (6), we can establish the conditions over the temporal duration of the impulse modulation response to reduce the convolutional effects and enhance the system performance. Therefore, we achieve an all optical AWG independently of the temporal impulse response.

From above assumptions, we conclude that independently of a negligible or considerable dispersion over the input pulse (i.e., $|\varphi_2| \ll \sigma_0^2$ *or* $|\varphi_2| \gg \sigma_0^2$, respectively), the first term of Eq. (5) prevails over the second one. Comparing with schemes based on linear incoherent optical signal processing, this fact is illustrated by the condition $|\varphi_2| \gg \sigma_0\sigma_c$ which ensures a proper performance of the system [5] since the second-order dispersion is neglected. In this way, nonlinear incoherent optical processing brings advantages compared to coherent techniques which must fulfill $|\varphi_2| \gg \sigma_0^2$ according to the dispersion requirements where only the pulsewidth σ_0 is involved [10, 11]. Comparing both coherent and incoherent conditions, when a similar pulsewidth is considered, incoherent processes need smaller dispersion values since $\sigma_0 \gg \sigma_c$. For typical dispersion values of around of hundreds of ps^2, coherent schemes have to reduce the pulsewidth significantly making difficult the performance when an external modulation is involved. In fact, generally coherent techniques make use of pulsed lasers around hundreds of femtoseconds [11, 12] operating directly in the optical domain.

In principle, the use of incoherent light processing is related to applications requiring high signal-to-noise ratio [17]. In structures proposed for AWG with incoherent optical sources, this fact gives as a result intensity fluctuations of the optical field associated to the generated output waveform [5]. Nevertheless, we have experimentally demonstrated that this restriction can be overcome through a proper average of the output waveforms [7]. However, an averaging process could be considered a restriction for real-time applications. In this sense, high values of SNR have been recently achieved by reducing drastically the number of averaging events by the introduction of low-noise figure devices in the system, such as an incoherent broadband light source, based on cascading an superluminiscent laser diode and an semiconductor optical amplifier [19] or the use of a suitable photodetection scheme based on differential configuration [20].

3. Numerical results and discussion: generation of chirped pulses

In order to evaluate the proposed technique, we consider the adaptation of the scheme shown in Fig. 1 for the generation of chirped electrical arbitrary waveforms. For this purpose, we consider an incoherent optical source power distribution, P(ω), which is sliced with a periodicity of Δω by means an interferometric structure T(ω) as follows:

$$T(\omega) = \frac{1}{2}\left[1+\cos\left(2\pi\frac{\omega}{\Delta\omega}\right)\right] \tag{7}$$

Thereby, the resulting optical source power spectral distribution S(ω), previously considered, is given by spectrum S(ω) = P(ω)·T(ω). Now, assuming conditions of Eq. (6) and introducing Eq. (7) into Eq. (5), the generated waveform at the output of the system can be written as:

$$I_{OUT}(t) = \frac{I_o}{4\pi}\frac{P(\omega)}{\underbrace{|\varphi_2+\varphi_3\omega|}_{r(t)}}\Bigg|_{\omega=\omega_m} \cdot \left[1+\cos\left(\underbrace{2\pi\frac{\omega}{\Delta\omega}}_{\Psi(t)}\right)\right]\Bigg|_{\omega=\omega_m} \tag{8}$$

As we observe, this signal can be described by an envelope r(t) and a time-dependent phase term ψ(t) depending on the nonlinear relationship given by Eq. (4) which performs the

#162085 - $15.00 USD Received 25 Jan 2012; revised 13 Feb 2012; accepted 17 Feb 2012; published 7 Mar 2012

chirp characteristic. Indeed, the instantaneous frequency can be obtained by the first-order derivative of the time-dependent phase term ψ(t) as follows:

$$f_{ins}(t) = \frac{1}{2\pi}\frac{d\psi(t)}{dt} = \frac{f_o}{\sqrt{1+2\frac{\varphi_3}{\varphi_2^2}t}} \qquad where \qquad f_o = \frac{1}{|\varphi_2|\Delta\omega} \tag{9}$$

where f_o corresponds to the central frequency of the generated signal, i.e. when t = 0.

As an example, a Gaussian profile P(ω) with a 3-dB optical bandwidth of $2\pi\cdot 10$ THz (80 nm) is plotted in Fig. 2(a). In addition, a sinusoidal slicing T(ω) is considered with a periodicity $1/(2\pi)$ THz (Fig. 2(b)) given the optical source spectrum S(ω) shown in Fig. 2(c). The modulator impulse response $h_{mod}(t)$ is defined through a Gaussian pulse with width σ_0 = 25 ps. The first- (φ_2) and second-order (φ_3) dispersion are chosen to be −200 ps^2 and 2 ps^3, respectively, which values are close to conventional single-mode fibers (SMF) or dispersion-compensating fibers (DCF). Note as, in this case, the electrical input pulse is not affected by the second-order dispersion since the condition $\sigma_0 \gg |\varphi_3/\varphi_2|$ is widely satisfied. The resulting waveform has been plotted in Fig. 2(d) showing an envelope according to the optical source power distribution close to a Gaussian pulse with a full width half maximum (FWHM) of 12 ns and a slight asymmetry due to the second-order dispersion considered [12]. The instantaneous frequency of the pulse within the FWHM (●) has been obtained by the reciprocal of the time period and is also plotted in Fig. 2(d) showing a negative chirped behavior from 4 to 7.75 GHz around a central frequency f_o of 5 GHz.

Next, the second-order dispersion has been changed to be −2 ps^3 and the results are shown in Fig. 2(e). As can be observed, in this case, the behavior of the generated waveform is opposite to the one shown in Fig. 2(d) both in terms of the envelope and the instantaneous frequency. In both cases shown in Figs. 2(d) and 2(e), the TBWP is around 45. Note that, compared to coherent approaches based on nonlinear frequency-to-time mapping [11, 12], the control of the pulsewidth of the generated waveform permits to improve in one order of magnitude the TBWP using similar values of second-order dispersion involved in experimental implementation. In addition, we have added in Figs. 2(d) and 2(e) the theoretical prediction of the instantaneous frequency according to Eq. (9) and we can observe an excellent agreement with the values obtained directly by the waveform.

Comparing the optical spectrum S(ω) of Fig. 2(c) with the generated waveforms in Figs. 2(d) and 2(e), we emphasize that the effects of the convolution in Eq. (5) are practically negligible. In fact, taking into account that for a sliced source the coherence time can become approximated by $\sigma_c \sim 1/\Delta\omega$, the conditions shown in Eq. (6) are fulfilled for the values used in simulation.

#162085 - $15.00 USD Received 25 Jan 2012; revised 13 Feb 2012; accepted 17 Feb 2012; published 7 Mar 2012

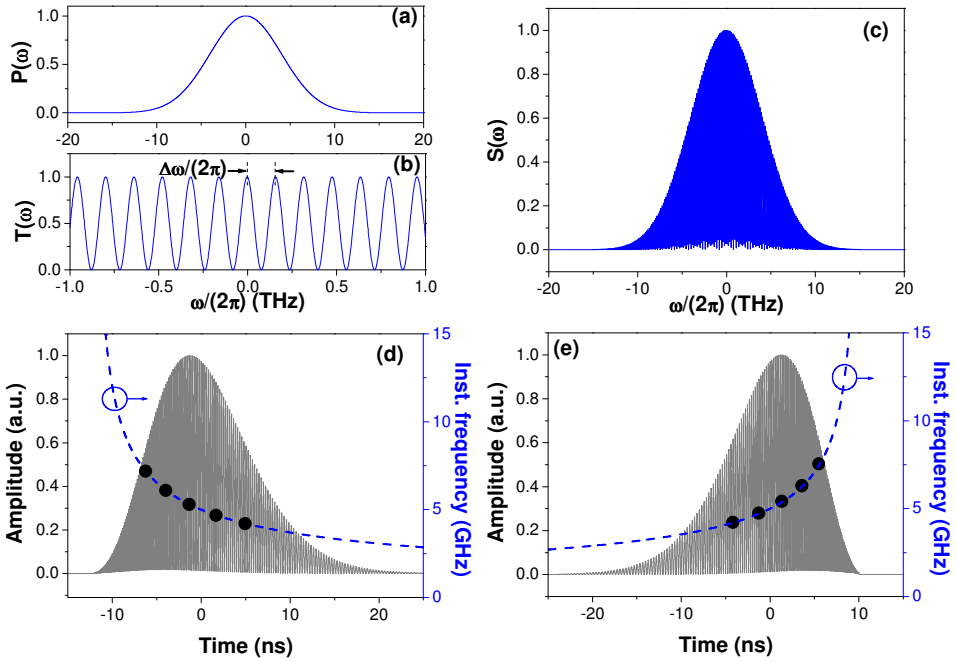

Fig. 2. (a) Gaussian profile P(ω) and (b) slicing T(ω) of a periodicity 1/(2π) THz introduced to obtain (c) the optical source power distribution S(ω). Microwave pulse generated (grey line) and its instantaneous frequency (●) for second-order dispersion (d) $\varphi_3 = 2$ ps^3 and (e) $\varphi_3 = -2$ ps^3. Theoretical prediction of instantaneous frequency included in dashed line.

The reconfigurability of the waveform envelope can be carried out by the control of the optical source power spectral distribution according to Eq. (5). Now, we set a uniform optical spectrum S(ω) as shown by the inset of Fig. 3(a). The generated waveform and its corresponding instantaneous frequency have been plotted in Fig. 3(a). The signal characteristics in terms of FWHM and instantaneous frequency behavior are similar to the one shown in Fig. 2(e) maintaining a TBWP around 45. Nevertheless, the envelope of the waveform has been changed since we are using an optical source with a uniform profile. In this case, we can distinguish two different effects over the waveform envelope: the asymmetry due to the second-order dispersion in the non-linear frequency-to-time mapping process and the effect of the local dispersion over S(ω) at each optical frequency ω.

Furthermore, the central frequency of the generated waveform depends on the slicing of the optical source power distribution according to Eq. (9). We set an optical source spectra with a periodicity of 1/(4π) THz giving the generated waveform and the corresponding instantaneous frequency plotted in Fig. 3(b). As can be observed from the instantaneous frequency graph, a variation from 8 to 15.5 GHz is existing with the central frequency around 10 GHz. In our experimental proof [15], we performed the slicing process by a Mach-Zehnder Interferometer (MZI) which permits to realize a continuous frequency tuning in contrast with other techniques existing in the literature that make use of other inflexible interferometric structures as Sagnac-Loop Filters [11, 12]. Moreover, as can be observed from Fig. 3(b), the envelope of the waveform shows an accurate uniform profile since we have set a suitable profile plotted in the inset of Fig. 3(b), maintaining a FWHM around 12 ns. In this case, the TBWP achieved is around 90. Therefore, the control over the waveform using the optical source permits to avoid the effects of the second order dispersion in the frequency-to-time process and the local dispersion over S(ω) at each optical frequency ω. Note that coherent systems usually generate Gaussian waveforms since the femtosecond pulsed lasers have a broadband transform-limited ultrashort Gaussian spectrum and shaping to a different profile

#162085 - $15.00 USD Received 25 Jan 2012; revised 13 Feb 2012; accepted 17 Feb 2012; published 7 Mar 2012

involves a non-efficient use of the available power spectral density [11–13]. Besides, the easy reconfiguration of the waveform envelope directly in the optical domain is in contrast with other approaches based on incoherent processing where the control of the waveform envelope is carried out electrically by an external modulation [14].

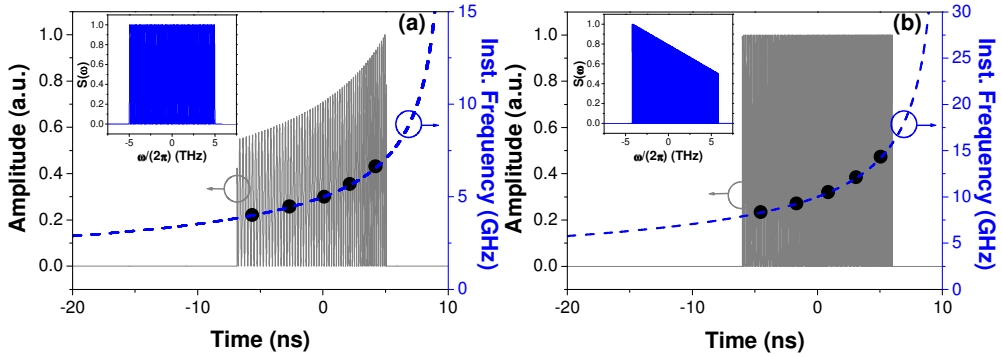

Fig. 3. Generated waveform (grey line) and instantaneous frequency (●) for (a) 5 GHz and (b) 10 GHz central frequencies where the optical source power distribution corresponds to a uniform (Inset a) and compensated uniform (Inset b) profiles, respectively. Instantaneous frequency theoretical prediction (dashed line).

As we have shown, the capacity of generating arbitrary signals is related to the capacity of reconfiguration that the system offers by controlling the power spectral density of the optical source. In contrast, a large TBWP is mainly referred to the available optical bandwidth. Therefore, the input optical source can be considered as the key element of the structure to enhance an envelope reconfigurability and TBWP control. The input optical source of the system can be implemented by combining a broadband optical source and a programmable optical filter which determines the optical power spectral distribution S(ω). We can find commercial devices as optical channel selectors [7] or optical power shapers based on two-dimensional liquid crystal on silicon (LCoS) pixel array [21] in order to control the profile with a high flexibility. Regarding the reconfiguration time of the waveforms generated, the response time is given by the programmable optical filter which is limited to to milliseconds. Nevertheless, previous configurations related to reconfiguration switching offer the possibility of using the electrical modulation pulse at high rates to incorporate flexibility to the system [22, 23]. This key idea permits to implement alternative structures by combining the incoherent optical processing using nonlinear dispersive elements and the fast reconfiguration switching in order to achieve a fast reconfigurable AWG in the range of several hundreds of picoseconds.

4. Conclusions

In this paper, we have proposed a novel technique based on the incoherent processing of a broadband optical signal through a nonlinear dispersive element for the generation of microwave arbitrary waveforms. As far as we are aware, this is the first time that a nonlinear relationship is set between the power spectral density of the optical source and the generated microwave pulse. A theoretical analysis of the system has been developed to obtain a detailed expression for the generated signal. In order to evaluate the performance of the system we have focused on the generation of chirped pulses. In this sense, we have demonstrated the control of the pulse characteristics in terms of chirp, envelope and central frequency by means of the second-order dispersion and the optical source power distribution. In this sense, the use of a broadband optical source allows us to increase the TBWP up to 90, and therefore, improving in more than one order of magnitude the values experimentally achieved by coherent processes using typical dispersion. Moreover, the direct reconfigurability of the

#162085 - $15.00 USD Received 25 Jan 2012; revised 13 Feb 2012; accepted 17 Feb 2012; published 7 Mar 2012

signal in the optical domain adds flexibility to the system since no electrical processes are involved.

Acknowledgments

The research leading to these results has received funding from the national project TEC TEC2011-26642 (NEWTON) funded by the Ministerio de Ciencia y Tecnología, the regional project PROMETEO GVA 2008/092 MICROWAVE PHOTONICS and the complementary grant for I + D projects for quality groups by Generalitat Valenciana ACOMP/2010/196.

#162085 - $15.00 USD Received 25 Jan 2012; revised 13 Feb 2012; accepted 17 Feb 2012; published 7 Mar 2012